Rapid Prototyping of Reconfigurable Microfluidic Channels in Undercooled Metal Particle-Elastomer Composites

*Boyce S. Chang[1]‡, Mario Fratzl [2,4]‡, Andrea Boyer[3], Andrew Martin[1], Henry C. Ahrenholtz[1], Isabelle De Moraes[4], Jean-Francis Bloch[5], Nora M. Dempsey[4], Martin M. Thuo[1]**

[1]Department of Materials Science and Engineering, Iowa State University, Ames, IA 50011, USA

[2]Univ. Grenoble Alpes, CNRS, Grenoble INP†, G2Elab, 38000 Grenoble, France

[3]Department of Mechanical Engineering, Iowa State University, Ames, IA 50011, USA

[4]Univ. Grenoble Alpes, CNRS, Grenoble INP†, Institut Néel, 38000 Grenoble, France

[5]Univ. Grenoble Alpes, CNRS, Grenoble INP†, 3SR, 38000 Grenoble, France

† Institute of Engineering Univ. Grenoble Alpes

*To whom correspondence should be addressed: mthuo@iastate.edu

KEYWORDS

microfluidics, undercooled particles, composites, rapid prototyping, ST3R

ABSTRACT

Conventional fabrication of microfluidic channels/devices are faced with challenges such as single use channels and/or significant time consumption. We propose a flexible platform for fabricating microfluidic channels simply through indentation on a smart composite—the so-called ST3R (Stiffness tuning through thermodynamic relaxation) composite. The application of ST3R composite allows rapid fabrication of microfluidic channels by hand or with a prefabricated stamp, and precise prototyping of complex designs using a 2D plotter. Indenter geometry, applied stress, filler loading, and number of repeated indentations affect channel dimensions and/or shape. These channels further exhibit; i) Substantial improvement against swelling by organic solvent, in part due to the high modulus of the solidified metal network. ii) Channel reconfigurability by heating the solidified undercooled metals. ST3R composite slabs have the potential to serve as microfluidic 'breadboards', from which complex channels can be integrated in a flexible manner.

INTRODUCTION

Fabrication of microfluidic devices has largely relied on soft lithography.[1, 2] Although robust, this method is typically limited to 2D channels, with the exception of stacked devices, which creates a multi-dimensional network. Soft lithography includes numerous patterning techniques,[3] including replica molding,[4] microtransfer molding,[5] solvent-assisted micromolding[6] or decal transfer lithography.[7] The most commonly used mold material is the epoxy-based negative photoresist known as SU-8, which allows for high-aspect-ratio microstructures.[8] Fabrication of the SU-8 molds, however, requires costly fabrication techniques. Alternatively, dry film SU-8 photoresist[9] were fabricated by lamination of commercial dry film photoresist on a planar

substrate. The latter method does not require a cleanroom, albeit with restrictions in sophistication or reconfigurability.

Recently, CAD assisted fabrication techniques have begun to break these fabrication barriers, allowing for improved micro-fluidic prototyping. These methods include: i) Xurography,[10] which uses a cutting or laser plotting tool and adhesive films to generate microfluidic structures. Conversely, this method is limited in terms of channel size and resolution. ii) Micromilling[11] uses a high precision but expensive computer numerical controlled (CNC) motion system. Additional constraints in material type exist due to variation in thermal and mechanical properties. iii) The most promising emerging technology is 3D printing, a method that allows direct fabrication of 3D microchannels in a single step.[12] 3D printing, however, requires expensive high resolution printing systems. Despite the range of tools available for microfluidic channel fabrication, supporting technology and/or versatility are the biggest bottlenecks to their adoption.

Embossing/debossing of soft materials, such as cellulose, has emerged as a simple and cost-effective method for fabricating microfluidic channels.[13-15] Soft materials often display distinct physical behaviors on the micro- and mesoscopic scale. These nonlinear effects are especially desirable for microfluidic systems, which are length scale dependent.[16] On the other hand, variable properties could complicate predictability, thus further challenging device fabrication. More recently, reconfigurable microfluidic channels were made from low melting point metals through so-called MnM (melt-n-mold) fabrication.[17] Through integration of soft materials with low melting point metals, we report a low-cost, rapid prototyping, and reusable microfluidic platform that does not require advanced fabrication tools. Based on the recently reported smart composites characterized by Stiffness Tuning Through Thermodynamic Relaxation (so-called ST3R

composite),[18] we present a microfluidic breadboard in which channels can be indented using a blunt object (e.g. a pen) in a matter of seconds.

RESULTS AND DISCUSSION

The ST3R composite consists of core-shell undercooled liquid metal particles[19, 20] embedded in an elastomer matrix (Figure 1a). In this work, we applied Field's metal undercooled particles incorporated into PDMS (polydimethylsiloxane). Upon indenting the surface of the composite using the tip of a pen, the particles in vicinity deform and solidify. This causes local changes in stiffness, which locks the matrix into a shape analogous to the applied stress field. Figure 1b shows a cross-section of the indented channel that is 9 μm deep. Scanning Electron Microscopy (SEM) images of the composite illustrate how mechanical deformation of the initially spherical particles occurs with concomitant solidification (Figure 1c-d). The fabricated channels, which have ridge-like structures on their sides (Figure 1e), are comparable to those obtained by other indentation methods.[21] Using the ST3R composite, channels can be made *via* different approaches including; i) hand-writing, which allows instant with concomitant access to virtually any design (Figure 1a), ii) stamping with a pre-fabricated stencil for rapid prototyping (Figure 1f), and iii) 2D plotting for greater precision and speed (Figure 1g). In this case, channel depth is varied through number of indenting passes or applied force (Figure 1h). The softer, 30% filler loading, composite continues to deform following repeated passes, with the increase in channel depth flattening out after *ca.* 10 passes. It should be noted that hand drawn, or stencil made channels can be made up to 30-40 μm deep depending on the applied load. Details on composite deformation as a function of stress can be found in our previous work.[18]

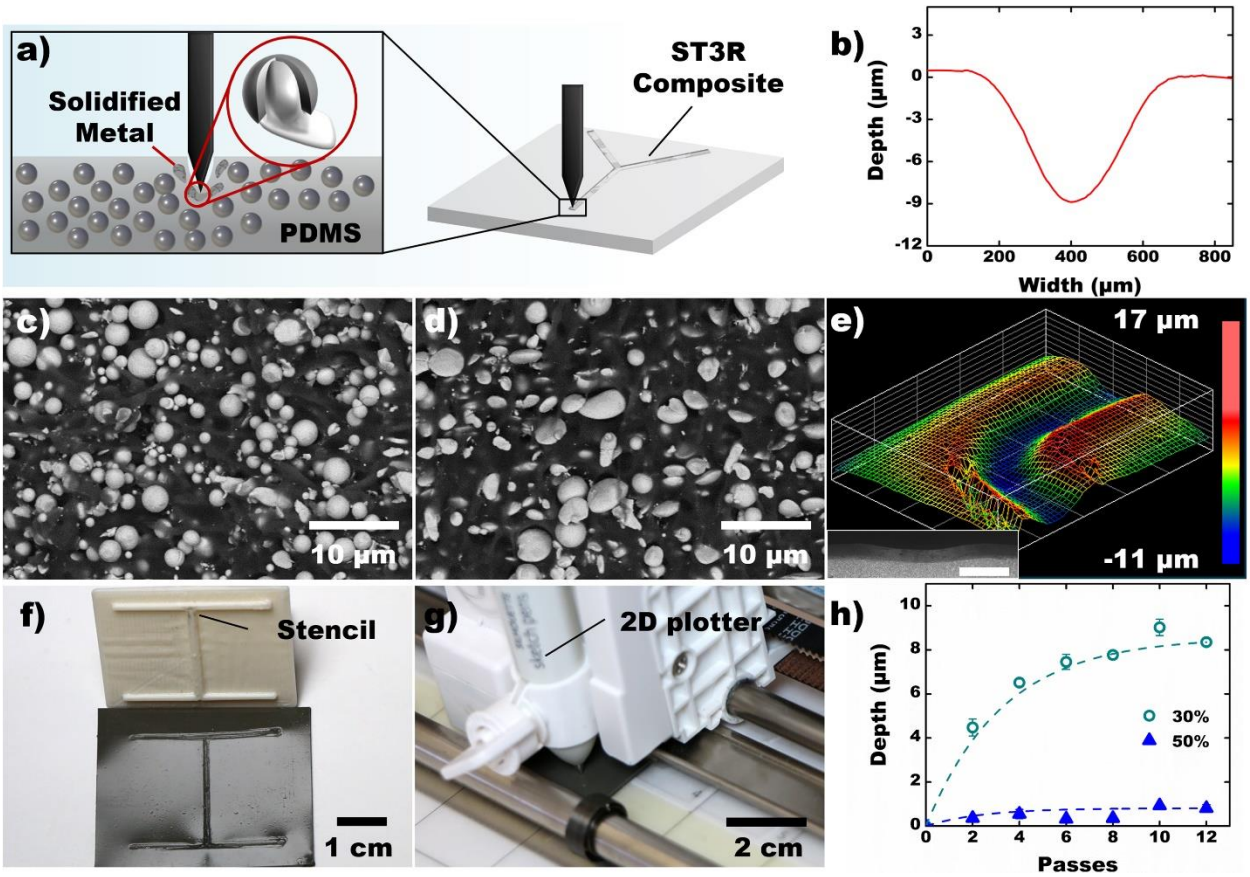

Figure 1. a) Schematic illustration of microchannels derived from ST3R composite by indentation. b) 2D depth profile of formed channels. c-d) Scanning electron microscopy of the composite (30% filler volume) cross-section before and after indenting in the vertical direction. e) 3D topographic heat map generated using contactless profilometer. Inset shows a low magnification SEM image of the channel (Scale bar = 500 μm). Channels formed using f) a 3D printed stencil, and g) a 2D plotter. h) Controlling channel depth by varying the number of passes on the 2D plotter on composites with different volume percent of undercooled metal fillers.

Besides applied pressure or number of passes over a given channel, depth also depends on percentage of filler, whereby 50% composite becomes unresponsive after the first indentation (Figure 1h). Increasing the filler content raises the local modulus up to 300%, which in turn modifies the deformability of the elastomer following successive passes.[18] This stiffening effect

occurs due to solidification of the undercooled liquid metal and concomitant welding of neighboring particles, leading to the formation of metal networks throughout the composite. Therefore, ST3R composites (E~15-80 MPa) should withstand 20-30 times higher flow pressure compared to conventional PDMS (E~0.5-3.7 MPa).[22] Finally, the indented channels are sealed with transparent tape to give a microfluidic device (Figure S1). The small channel depth ensures a Reynolds number, Re, < 1, giving rise to laminar flow (Figure 2a).

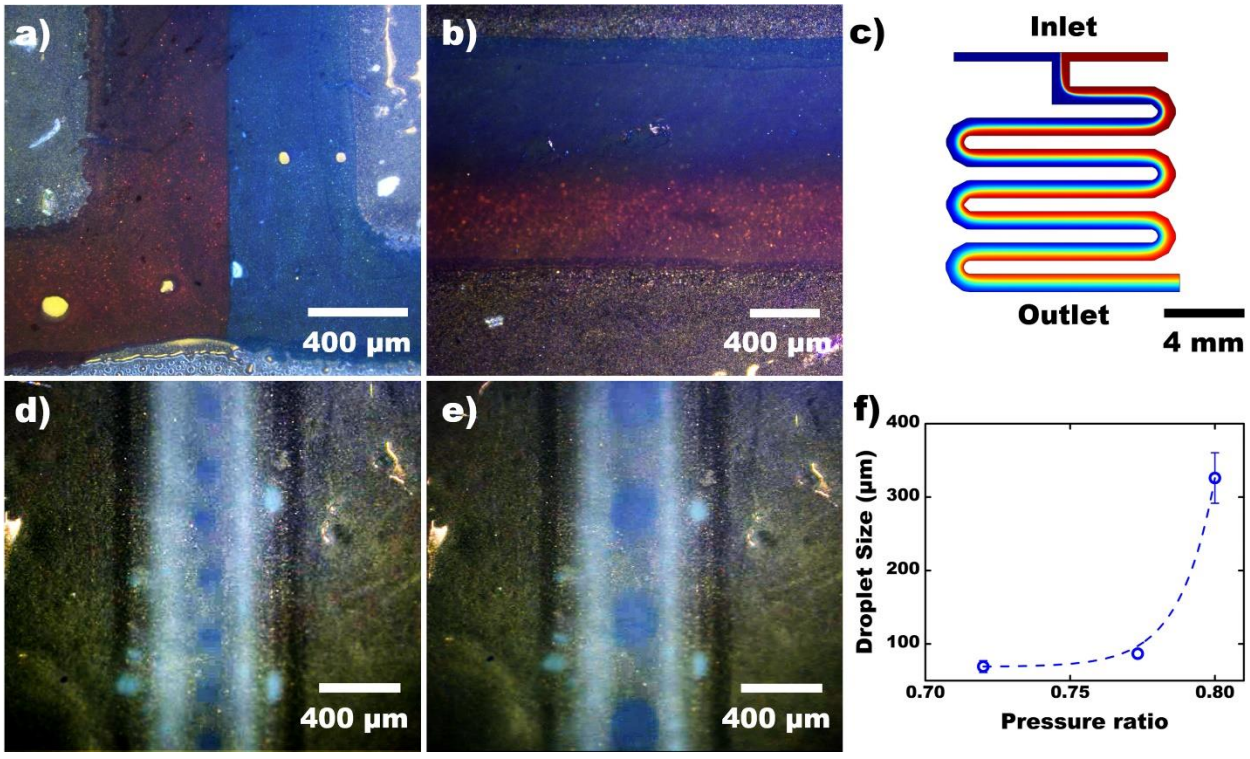

Figure 2. a) T-shaped channel showing laminar flow of dyed water. b) Center of a meander channel (mixer) in which blue and red dyed water are flowing. c) COMSOL simulation of meander channel. d-e) Droplet generation using a nozzle type channel. f) Controlling droplet size by tuning the water-oil pressure ratio.

The device was then connected to a pressure driven microfluidic pump (see Supporting information, Figure S2). To demonstrate versatility, we fabricated examples of well-known

microfluidic architectures. First, to show microfluidic diffusion-driven mixing behavior under lamina flow (low Re), we prepared a 90 mm long meander type mixer with two inlets and one outlet.[23] At the inlet, red and blue dyed fluids were injected at constant pressure (120 mbar). Simulations and experimental results, as expected, showed dye mixing at the interface of the two streams (Figure 2b-c). Thus, pen-based indentation resulted in functional microfluidic channels that did not introduce any unexpected fluid turbulence or pressure peaks. In a second demo, we fabricated a 3-way nozzle design (see Supporting information Figure S3). When the liquids have the comparable surface tension, a three-stream system is generated (see Supporting information Figure S3b) with liquid from the central inlet (red) flanked by streams from the outer channels (blue), as predicted *in silico* (Figure S4). Replacing the fluid in the center with a lower surface tension fluid (e.g. oil when water is on the outer channels), the configuration becomes a flow-focusing droplet generator (Figure S3a and S5). We obtained monodisperse droplets and, as expected,[24] achieved control over droplet size by changing the pressure ratio between water and oil (Figure 2d-f). Finally, we demonstrated the applicability of fabricated micro-channels in particle separation.[25] Separation is achieved by introducing a magnetic particle suspension on one side and an aqueous fluid on the other side of a T-channel junction. Using an external permanent magnet, we diverted the magnetic particles from the left side channel and trapped them on the right side. After removal of the permanent magnet, particles were readily washed away (Figure S6). Using this approach, ST3R composites could be used to develop new magnetic bead-based microfluidics.[26] In summary, we demonstrated the potential of indented ST3R composites for rapid prototyping of various types of microfluidic systems such as mixers, droplet generators or particle sorters.

A major caveat in PDMS-based microfluidics is its incompatibility with organic solvents due to swelling and delamination. Ability of ST3R composite to change filler geometry and stiffness upon activation can mitigate deformations due to solvent-driven hygrothermal stress. We, therefore, hypothesized that the presence of a metal particle network in activated ST3R composite would significantly dampen the effect of PDMS swelling, hence mitigate delamination and channel constriction. Swelling experiments in hexane—a good solvent for PDMS[28, 29]—were performed to verify the stability of ST3R composites (Figure 3). Native PDMS, as expected, showed >2x elongation due to swelling compared to ST3R composite. We infer that chain mobility in PDMS is significantly hindered by the presence of the stiff filler material in ST3R. Thus, the diffusion of solvent molecules is retarded due to restricted chain reorganization.[27] The improved resistance of the ST3R composite to deformation under solvent stress could potentially expand applications of PDMS- or other elastomer-based microfluidics beyond aqueous systems/analytes.

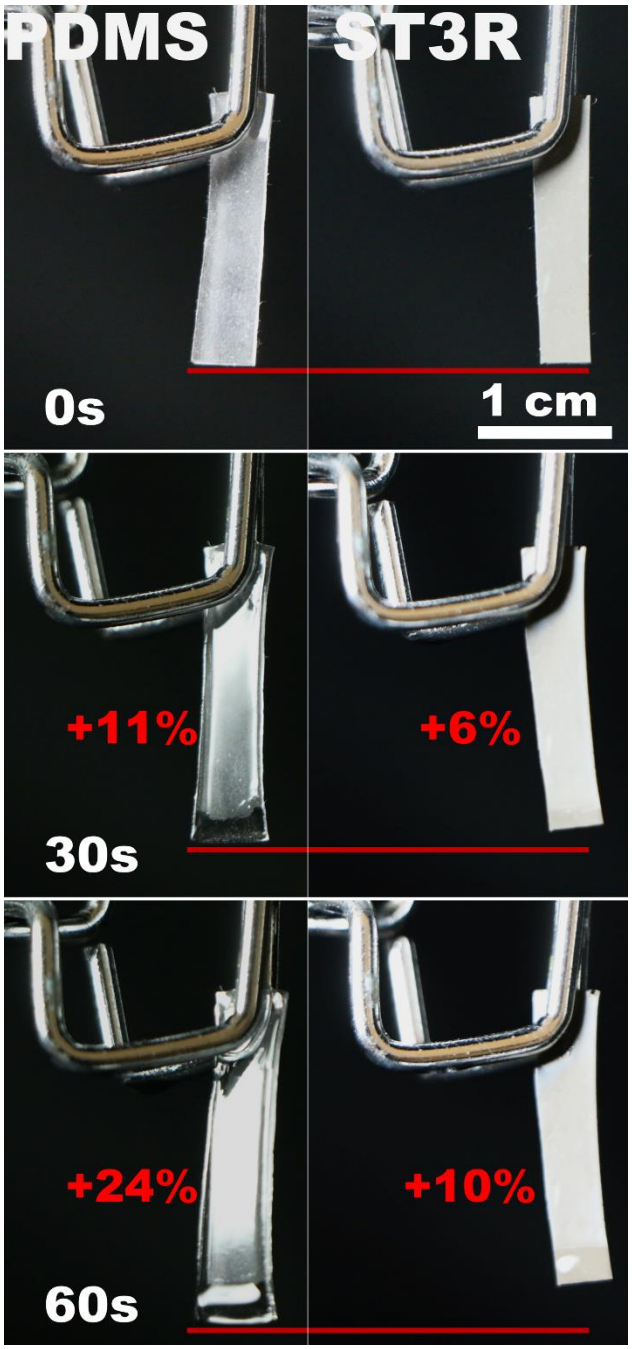

Figure 3. Comparison of the degree of swelling of PDMS and ST3R composite (50% volume), following different exposure times in hexane.

The use of low melting metals also creates an opportunity for reconfigurable channels.[17] This is achieved by re-melting the metal (in this case at T ≥62˚C), which anchors the shape of the channels. The elastomer matrix relaxes as the metal melts, partly reverting to its un-indented shape. We

hypothesize that complete shape memory is not thermodynamically feasible (limitations of the second law of thermodynamics) due to entropic constraints associated with phase transition and matrix relaxation/reconfiguration. Figure 4a shows the topology of a new channel indented over a reconfigured channel. This data illustrates; i) reduced depth of the old channel, and ii) a deeper new channel (Figure 4a). Due to capillary forces, fluids passing across the new channel do not leak into the old channel, confirming the reusability of the composite-based microfluidic device (Figure 4b). We further verify this by running brine solution and show that NaCl precipitates exclusively in the new channel (Figure 4c-e). Small amounts of adventitious salt are found in the reconfigured channel due to accidental deposition when removing the sealing tape to reveal the surface for SEM. A caveat with heat-induced reconfiguration lies in the concomitant alterations on the surface oxide of the metal,[30] which can alter the properties of the composite upon repeated reuse. Furthermore, applications that require elevated temperatures could induce undesired deformation in the composite. Nonetheless, alloys with higher melting point than Field's metal (e.g. BiSn) [19] can be processed into undercooled liquid metal particles, thus increasing the operation temperature of the composite.

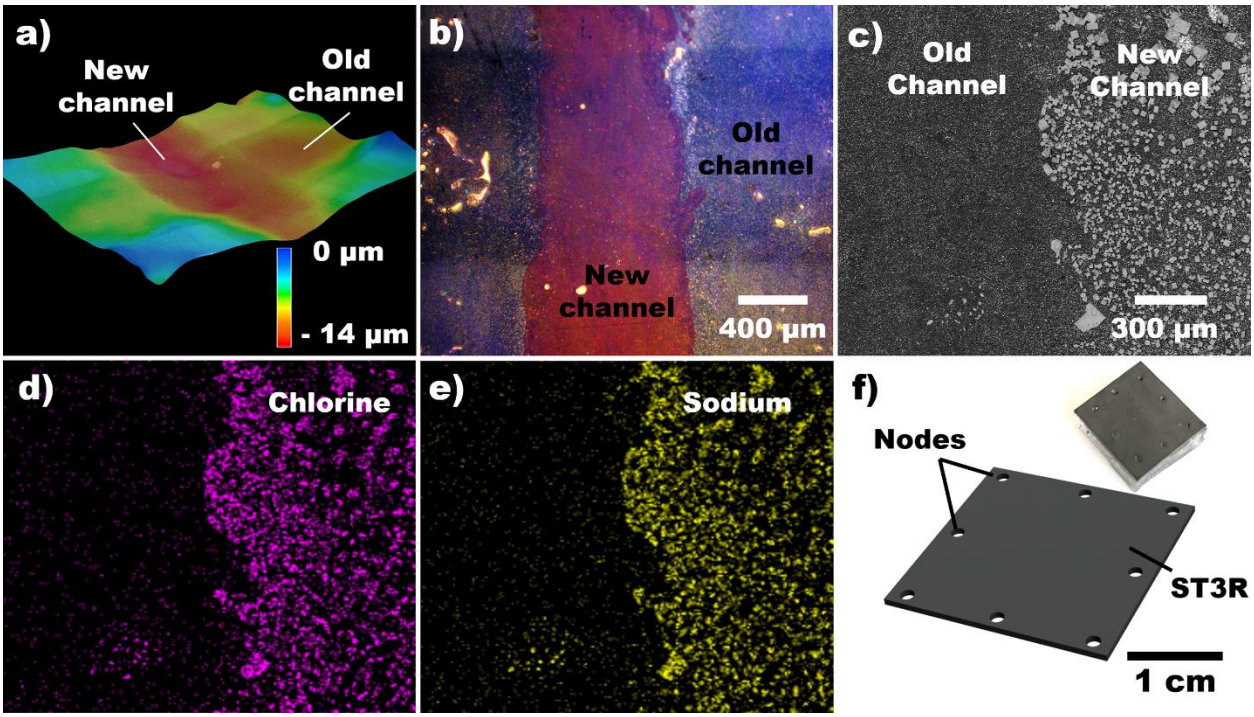

Figure 4. a) Reusability demonstrated by heating (>62˚C) a composite containing a channel and subsequently drawing a new channel in the perpendicular direction, at room temperature. b) Demonstration of dyed water flowing through the new channel. c-e) SEM micrograph and corresponding energy dispersive X-ray spectroscopy map of NaCl precipitated from salt solution restricted at the new channel. f) Prototype of a microfluidic breadboard using an ST3R composite.

Finally, we demonstrate that ST3R composites can be used as microfluidic 'breadboards' analogous to those in the electronic industry. These 'breadboards' allow for simple and reversible channel preparation by drawing making them versatile tools in point-of-use devices. This is illustrated by fabricating a 20 mm x 20 mm ST3R composite that is fixed on a large PDMS slab support. Multiple inlets and outlets are pre-drilled on the edge of the laminate structure (Figure 4f). The resulting microfluidic breadboard allow users to prototype any microfluidic channel with ease (by hand) using a pen. The nodes can be interconnected as desired, creating channels of any complexity. After usage, the substrate can then be erased through heating and reused. This allows

for rapid prototyping and iterative development of microfluidic devices on an office desk, in the field, or in resource-limited settings, eliminating the need for advanced or complicated fabrication facilities. Compared to conventional PDMS micro-channel fabrication techniques, systems designed on such breadboards are much easier to setup, test and correct. Furthermore, drawn channels are not simply extruded 2D patterns but have rounded cross sections (Figure 1e),[31] mimicking the rheology in small channels (leading to a more accurate representation of for example biological microenvironments)[32] and maximizing flow rate for a given pressure and channel dimension.[33]

CONCLUSION

In conclusion, we demonstrate that ST3R composites constitute an excellent platform for fabricating microfluidic channels by providing the ability for instant, precision prototyping and rapid production of complex designs. The channel depth can be tuned by changing the number of indenting passes, applied force or filler loading. Furthermore, the presence of smart metal fillers significantly enhances structural stability in an organic solvent, a major challenge in conventional PDMS structures. The composite can also be reused by heating above the melting point of the filler metal. We envision that this composite could act as a 'breadboard' for microfluidics, analogous to electronic devices.

MATERIALS AND METHODS

Materials

Field's metal (eutectic indium (51%)-bismuth (32.5%)-tin (16.5%)) was purchased from Rotometals. Slygard 184 was purchased from Ellsworth Adhesives. Ethanol (>99.2%) was

purchased from Decon Laboratories Inc. Glacial acetic acid (99.7%) was purchased from Fisher Scientific. Diethylene glycol (99.9%) was purchased from VWR. Crisco® canola cooking oil and Tone's® food coloring was purchased from Walmart Inc. Sodium chloride (99%) was purchased from Fisher Scientific.

Characterization techniques

Surface profiles were obtained using a Zygo NewView 7100 Optical surface profilometer, coupled with a 5x objective lens. Scanning electron microscopy images were obtained using a FEI Quanta 250 FE-SEM in low pressure mode (100 Pa H_2O). Backscattered electron detector was used to distinguish between phases in the composite. Microfluidic channels were indented using a Silhouette Cameo® craft cutter (2D plotter). Optical micrographs were obtained using a Keyence Corporation VHX-1000 coupled with VH-Z100R/W lens.

Preparation of liquid metal core shell particles

The Shearing Liquids Into Complex Particles (SLICE) technique[19, 20, 34] was utilized to synthesize all core shell particles used in this work. For a typical experiment, 30 g of Field's metal was placed in a blender containing 100 ml of solvent (diethylene glycol containing 2% acetic acid). The blender was then heated to 175 °C using heat tape. Shearing was carried out for 7 minutes. The resulting grey solution was then filtered and rinsed using ethanol and ethyl acetate to remove residual solvent. Based on inspection by SEM, the particle size ranged from 1 – 10 μm.

Composite fabrication

Typically, core shell particles of desired amount were first filtered and partially dried in vacuum (particles were kept in ethyl acetate to prevent degradation). The desired amount was then added to premixed (10:1 ratio) Sylgard 184. 18 g of Field's metal undercooled particles were added into 5 g of Sylgard 184. This mixture was stirred gently with a spatula for at least 10 minutes or until a homogeneous mixture was achieved. The mixture was outgassed to form an isotropic homogeneous paste. The composite was then cured at 100°C for 12 hours using a glass mold (2.0 x 6.0 x 0.1 cm). The composite was analyzed by Differential Scanning Calorimetry to ensure undercooling was preserved. Slabs of 2.0 x 2.0 x 0.1 cm were diced using a razor blade and used to fabricate the channels.

Microfluidic channel fabrication and usage

Channels were printed onto the composite using a Silhouette Cameo® craft cutter. Designs were made using Silhouette Studio®. Inlet and outlet holes were made using a drilling tool. These holes were capped with syringe needles, which were connected to a pressure driven microfluidic pump using polypropylene tubes. The channels were sealed using a commercial TESA Pack® transparent tape.

Simulations

Numerical Multiphysics simulations were performed using COMSOL Multiphysics 5.2.

ASSOCIATED CONTENT

The Supporting Information is available free of charge on the ACS Publications website.

Device fabrication steps and example of a functional microfluidic setup, details on the 3-way type nozzle channel, COMSOL simulations of 3-way type nozzle and image of magnetic particles injected into channels.

AUTHOR INFORMATION

Corresponding Author

*mthuo@iastate.edu

Author Contributions

The manuscript was written with contributions from all authors. All authors have given approval to the final version of the manuscript. ‡These authors contributed equally.

Funding Sources

This work was supported by Iowa State University through startup funds and through a visiting professorship to MT from *laboratoire d'Excellence tec21* and *laboratoire 3SR*.

ACKNOWLEDGMENTS

BC, AM and MT are supported by Iowa State University startup funds. AB was supported by the IINSPIRE-LSAMP program. M.F. was supported by the French Ministry of Higher Education, Research and Innovation (MESRI, bourse doctorale ministérielle). Experiments were carried out at Iowa State University, CIME-Nanotec/ FMNT, 3SR and Institut Néel.

REFERENCES

(1) Duffy, D. C.; McDonald, J. C.; Schueller, O. J. A.; Whitesides, G. M., Rapid Prototyping of Microfluidic Systems in Poly(dimethylsiloxane). *Anal. Chem.* **1998,** *70*, 4974.

(2) Hofmann, O.; Niedermann, P.; Manz, A., Modular Approach to Fabrication of Three-Dimensional Microchannel Systems in PDMS—Application to Sheath Flow Microchips. *Lab Chip* **2001,** *1*, 108.
(3) Faustino, V.; Catarino, S. O.; Lima, R.; Minas, G., Biomedical Microfluidic Devices by Using Low-Cost Fabrication Techniques: A Review. *J. Biomech* **2016,** *49*, 2280.
(4) Xia, Y.; McClelland, J. J.; Gupta, R.; Qin, D.; Zhao, X.-M.; Sohn, L. L.; Celotta, R. J.; Whitesides, G. M., Replica Molding Using Polymeric Materials: A Practical Step Toward Nanomanufacturing. *Adv. Mater.* **1997,** *9*, 147.
(5) Zhao, X.-M.; Xia, Y.; Whitesides, G. M., Fabrication of Three-Dimensional Micro-Structures: Microtransfer Molding. *Adv. Mater.* **1996,** *8*, 837.
(6) King, E.; Xia, Y.; Zhao, X.-M.; Whitesides, G. M., Solvent-Assisted Microcontact Molding: A Convenient Method for Fabricating Three-Dimensional Structures on Surfaces of Polymers. *Adv. Mater.* **1997,** *9*, 651.
(7) Childs, W. R.; Nuzzo, R. G., Decal Transfer Microlithography: A New Soft-Lithographic Patterning Method. *J. Am. Chem. Soc.* **2002,** *124*, 13583.
(8) Abgrall, P.; Lattes, C.; Conédéra, V.; Dollat, X.; Colin, S.; Gué, A. M., A Novel Fabrication Method of Flexible and Monolithic 3D Microfluidic Structures Using Lamination of SU-8 Films. *J. Micromech Microeng.* **2005,** *16*, 113.
(9) Stephan, K.; Gabriela, B.; Michael, L.; Daniel, H.; Anja, B., Processing of Thin SU-8 Films. *J. Micromech Microeng.* **2008,** *18*, 125020.
(10) Bartholomeusz, D. A.; Boutte, R. W.; Andrade, J. D., Xurography: Rapid Prototyping of Microstructures Using a Cutting Plotter. *J. Microelectromech. Syst.* **2005,** *14*, 1364.
(11) Guckenberger, D. J.; de Groot, T. E.; Wan, A. M. D.; Beebe, D. J.; Young, E. W. K., Micromilling: A Method for Ultra-Rapid Prototyping of Plastic Microfluidic Devices. *Lab Chip* **2015,** *15*, 2364.
(12) Au, A. K.; Huynh, W.; Horowitz, L. F.; Folch, A., 3D-Printed Microfluidics. *Angew. Chem. Int. Ed.* **2016,** *128*, 3926.
(13) Thuo, M. M.; Martinez, R. V.; Lan, W.-J.; Liu, X.; Barber, J.; Atkinson, M. B. J.; Bandarage, D.; Bloch, J.-F.; Whitesides, G. M., Fabrication of Low-Cost Paper-Based Microfluidic Devices by Embossing or Cut-and-Stack Methods. *Chem. Mater.* **2014,** *26*, 4230.
(14) Oyola-Reynoso, S.; Frankiewicz, C.; Chang, B.; Chen, J.; Bloch, J. F.; Thuo, M. M., Paper-Based Microfluidic Devices by Asymmetric Calendaring. *Biomicrofluidics* **2017,** *11*, 014104.
(15) Fratzl, M.; Chang, B. S.; Oyola-Reynoso, S.; Blaire, G.; Delshadi, S.; Devillers, T.; Ward, T.; Dempsey, N. M.; Bloch, J.-F.; Thuo, M. M., Magnetic Two-Way Valves for Paper-Based Capillary-Driven Microfluidic Devices. *ACS Omega* **2018,** *3*, 2049.
(16) Bartolo, D.; Aarts, D. G. A. L., Microfluidics and Soft Matter: Small is Useful. *Soft Matter* **2012,** *8*, 10530.
(17) Li, Z.; Tevis, I. D.; Oyola-Reynoso, S.; Newcomb, L. B.; Halbertsma-Black, J.; Bloch, J.-F.; Thuo, M., Melt-and-Mold Fabrication (MnM-Fab) of Reconfigurable Low-Cost Devices for Use in Resource-Limited Settings. *Talanta* **2015,** *145*, 20.
(18) Chang, B. S.; Tutika, R.; Cutinho, J.; Oyola-Reynoso, S.; Chen, J. H.; Bartlett, M. D.; Thuo, M. M., Mechanically Triggered Composite Stiffness Tuning through Thermodynamic Relaxation (ST3R). *Mater. Horiz.* **2018,** *5*, 416.
(19) Çınar, S.; Tevis, I. D.; Chen, J.; Thuo, M., Mechanical Fracturing of Core-Shell Undercooled Metal Particles for Heat-Free Soldering. *Sci. Rep.* **2016,** *6*, 21864.

(20) Tevis, I. D.; Newcomb, L. B.; Thuo, M., Synthesis of Liquid Core-Shell Particles and Solid Patchy Multicomponent Particles by Shearing Liquids Into Complex Particles (SLICE). *Langmuir* **2014,** *30*, 14308.
(21) Gong, J.; Lipomi, D. J.; Deng, J.; Nie, Z.; Chen, X.; Randall, N. X.; Nair, R.; Whitesides, G. M., Micro- and Nanopatterning of Inorganic and Polymeric Substrates by Indentation Lithography. *Nano Lett.* **2010,** *10*, 2702.
(22) Wang, Z.; Volinsky, A. A.; Gallant, N. D., Crosslinking Effect on Polydimethylsiloxane Elastic Modulus Measured by Custom-Built Compression Instrument. *J. Appl. Polym. Sci.* **2014,** *131*, 41050.
(23) Jiang, F.; Drese, K. S.; Hardt, S.; Küpper, M.; Schönfeld, F., Helical Flows and Chaotic Mixing in Curved Micro Channels. *AlChE J.* **2004,** *50*, 2297.
(24) Garstecki, P.; Gitlin, I.; DiLuzio, W.; Whitesides, G. M.; Kumacheva, E.; Stone, H. A., Formation of Monodisperse Bubbles in a Microfluidic Flow-Focusing Device. *Appl. Phys. Lett.* **2004,** *85*, 2649.
(25) Gijs, M. A. M., Magnetic Bead Handling On-Chip: New Opportunities for Analytical Applications. *Microfluid Nanofluidics* **2004,** *1*, 22.
(26) Rida, A.; Gijs, M. A. M., Manipulation of Self-Assembled Structures of Magnetic Beads for Microfluidic Mixing and Assaying. *Anal. Chem.* **2004,** *76*, 6239.
(27) Abraham, J.; Maria, H. J.; George, S. C.; Kalarikkal, N.; Thomas, S., Transport Characteristics of Organic Solvents through Carbon Nanotube Filled Styrene Butadiene Rubber Nanocomposites: The Influence of Rubber–Filler Interaction, The Degree of Reinforcement and Morphology. *Phys. Chem. Chem. Phys.* **2015,** *17*, 11217.
(28) Lee, J. N.; Park, C.; Whitesides, G. M., Solvent Compatibility of Poly(dimethylsiloxane)-Based Microfluidic Devices. *Anal. Chem.* **2003,** *75*, 6544.
(29) Atkinson, M. B. J.; Oyola-Reynoso, S.; Luna, R. E.; Bwambok, D. K.; Thuo, M. M., Pot-in-pot Reactions: A Simple and Green Approach to Efficient Organic Synthesis. *RSC Adv.* **2015,** *5*, 597.
(30) Cutinho, J.; Chang, B. S.; Oyola-Reynoso, S.; Chen, J.; Akhter, S. S.; Tevis, I. D.; Bello, N. J.; Martin, A.; Foster, M. C.; Thuo, M. M., Autonomous Thermal-Oxidative Composition Inversion and Texture Tuning of Liquid Metal Surfaces. *ACS Nano* **2018,** *12*, 4744.
(31) Hwang, Y.; Candler, R. N., Non-Planar PDMS Microfluidic Channels and Actuators: A Review. *Lab Chip* **2017,** *17*, 3948.
(32) Knowlton, S.; Yu, C. H.; Ersoy, F.; Emadi, S.; Khademhosseini, A.; Tasoglu, S., 3D-Printed Microfluidic Chips with Patterned, Cell-Laden Hydrogel Constructs. *Biofabrication* **2016,** *8*, 025019.
(33) De Ville, M.; Coquet, P.; Brunet, P.; Boukherroub, R., Simple and Low-Cost Fabrication of PDMS Microfluidic Round Channels by Surface-Wetting Parameters Optimization. *Microfluid Nanofluidics* **2012,** *12*, 953.
(34) Chang, B.; Martin, A.; Gregory, P.; Kundu, S.; Du, C.; Orondo, M.; Thuo, M., Functional Materials through Surfaces and Interfaces. *MRS Adv.* **2018,** *3*, 2221.

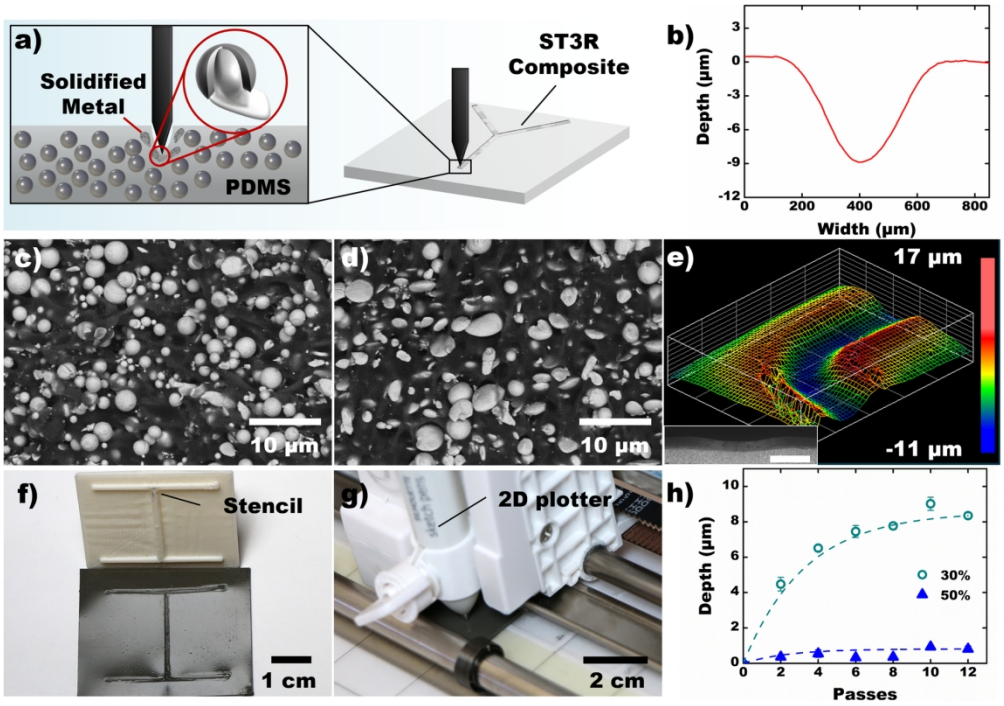

Figure 1. a) Schematic illustration of microchannels derived from ST3R composite by indentation. b) 2D depth profile of formed channels. c-d) Scanning electron microscopy of the composite (30% filler volume) cross-section before and after indenting in the vertical direction. e) 3D topographic heat map generated using contactless profilometer. Inset shows a low magnification SEM image of the channel (Scale bar = 500 μm). Channels formed using f) a 3D printed stencil, and g) a 2D plotter. h) Controlling channel depth by varying the number of passes on the 2D plotter on composites with different volume percent of undercooled metal fillers.

165x114mm (300 x 300 DPI)

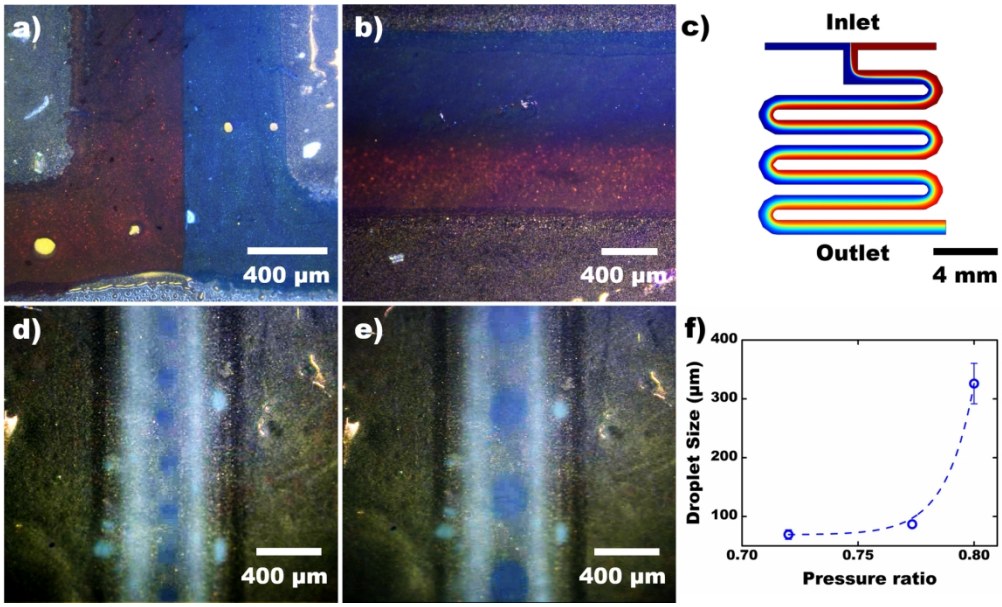

Figure 2. a) T-shaped channel showing laminar flow of dyed water. b) Center of a meander channel (mixer) in which blue and red dyed water are flowing. c) COMSOL simulation of meander channel. d-e) Droplet generation using a nozzle type channel. f) Controlling droplet size by tuning the water-oil pressure ratio.

165x98mm (300 x 300 DPI)

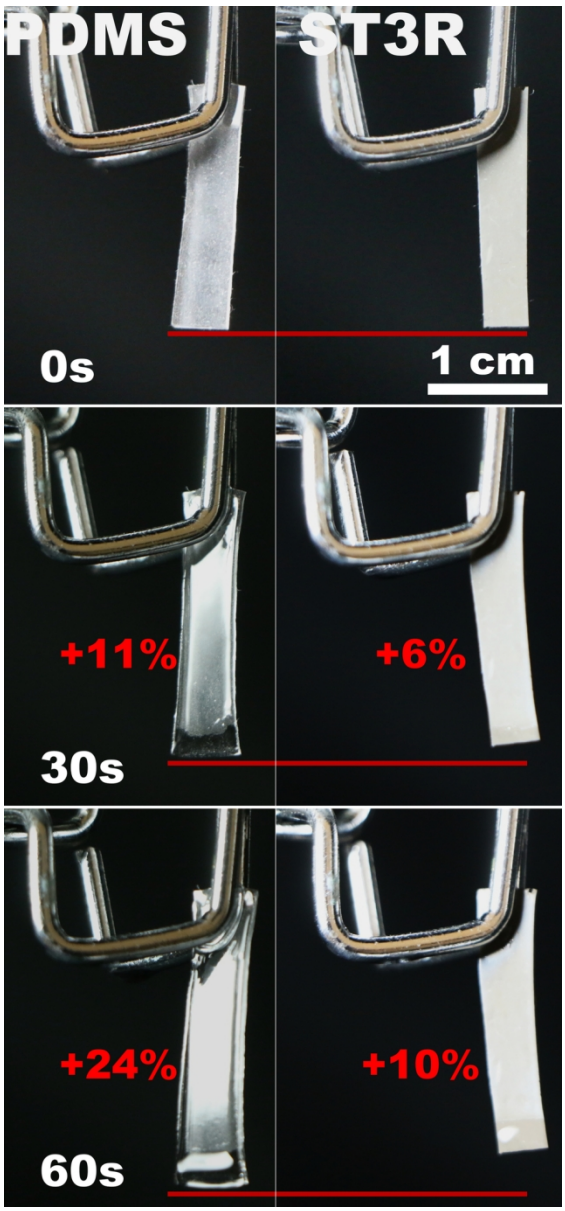

Figure 3. Comparison of the degree of swelling of PDMS and ST3R composite (50% volume), following different exposure times in hexane.

82x177mm (300 x 300 DPI)

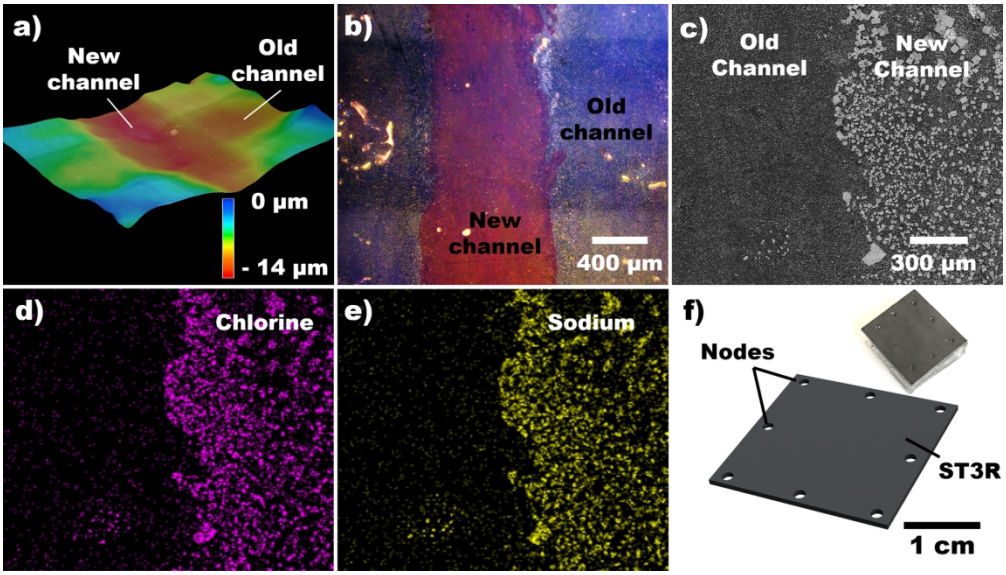

Figure 4. a) Reusability demonstrated by heating (>62°C) a composite containing a channel and subsequently drawing a new channel in the perpendicular direction, at room temperature. b) Demonstration of dyed water flowing through the new channel. c-e) SEM micrograph and corresponding energy dispersive X-ray spectroscopy map of NaCl precipitated from salt solution restricted at the new channel. f) Prototype of a microfluidic breadboard using an ST3R composite.

165x93mm (300 x 300 DPI)

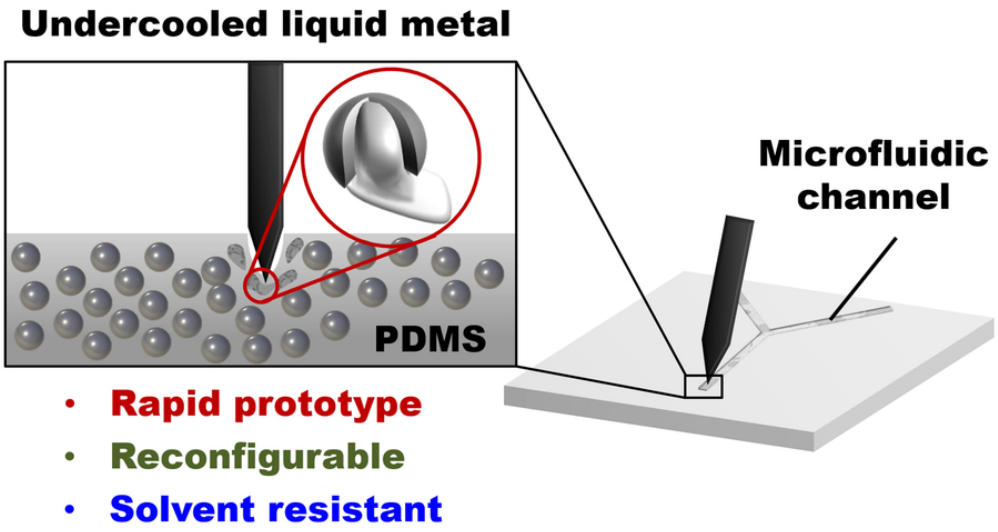

TOC

76x41mm (300 x 300 DPI)